Electrochemical Impedance Spectroscopy Investigation of Alloy Inconel 718 in Molten Salts at High Temperature

J.L. Trinstancho-Reyes[1,3], *M. Sanchez-Carrillo*[2], *R. Sandoval-Jabalera*[4], *V.M Orozco- Carmona*[1], *F.Almeraya-Calderón*[1], *J.G Chacón-Nava*[1] *and JG Gonzalez-Rodriguez*[5], *A. Martínez-Villafañe*[1,*]

[1] Centro de Investigación en Materiales Avanzados, S.C., Departamento de Integridad y Diseño de Materiales Compuestos. Miguel de Cervantes 120, Complejo Industrial Chihuahua, C.P. 31109, Chihuahua. Chih. México.
[2] Instituto Tecnologico de Durango, Departamento de Metal-Mecánica, Durango, Dgo., México
[3] Facultad de Ingeniería Mecánica. Universidad Tecnológica de Pereira. Pereira. Colombia
[4] Universidad Autónoma de Chihuahua, Facultad de Ingeniería. Chihuahua, Chih. México
[5] Universidad Autónoma del Estado de Morelos, FCQI-CIICAP. Cuernavaca-Morelos. México.
[*]E-mail: martinez.villafane@cimav.edu.mx

The corrosion behavior in molten salts of Inconel 718 (IN 718) superalloy was investigated by Electrochemical Impedance Spectroscopy (EIS). The corrosion test temperatures used were salt melting points of Na_2SO_4, $80V_2O_5-20Na_2SO_4$, $NaVO_3$ and natural ash (collected in a power plant). Different experimental runs were made attempting to establish the material behavior. The results showed that the corrosion process was controlled by activation and in some cases by diffusion. The aggressiveness of the salts increased with temperature, as indicated for the corrosion rates values derived. On the whole, the corrosion rates were somewhat similar at the lowest test temperatures. However at 588°C the $80V_2O_5-20Na_2SO_4$ salt showed a much higher corrosion rate than that recorded for Na_2SO_4 or natural ash. The results obtained from electrochemical measurements correlated well with those corrosion degradation observed by SEM, and comments on the behavior found are made.

1. INTRODUCTION

It is widely recognized that high temperature corrosion is a major cause of materials degradation in industrial processes involving gases or molten salts at high temperature. Apart from the traditional weight change technique to evaluate the degree of deterioration, good progress has been

done by using electrochemical techniques. Electrochemical impedance spectroscopy (EIS) is a technique which has been widely used in the study of aqueous corrosion, and has proved effective in determining and understanding reaction mechanisms and kinetics of corrosion processes. Only a limited number of EIS investigations conducted during molten-salt corrosion have been reported [1-11,16]. Farrell et al. [1] have employed the impedance technique to study the corrosion behavior of Nimonic 75 in Na_2SO_4 and in Na_2SO_4-1%NaCl at 750°C and 900°C. They observed that the shape of the impedance spectra has the characteristics of a diffusion-controlled reaction, which results because of the separation of the specimen from the gaseous environment by sample exposure to molten salts. By comparing the impedance at a fixed low frequency (50 mHz), the authors concluded that the corrosion rate was higher at 900°C than at 750°C or when sodium chloride was added to sodium sulfate. Gao et al. [2] also used this technique to ascertain the corrosion rate of Ni-Co alloys in Na_2SO_4 +10%NaCl. They observed a decline in the double layer resistance due to spallation of the oxide scale. Wu and Rapp [3] studied the hot corrosion of preoxidized Ni by a thin-fused Na_2SO_4 film at 1200°K (927°C) in a catalyzed $0.1\%SO_2$-O_2 gas mixture. By varying the specimen purity and preoxidation conditions for Ni, three distinct features of hot corrosion (passive, pseudo-passive, and active) were observed. Wu [5] further measured the double-layer capacitance at the preoxidized Ni/fused Na_2SO_4 interface. Similarly Wu et al. [4] have evaluated the corrosion resistance of commercial alloys in a Na_2SO_4-Li_2SO_4 salt mixture at 700°C by EIS and by weight loss, finding some degree of correlation among the techniques used. Wu [5] measured the double-layer capacitance at the preoxidized Ni/fused Na_2SO_4 interface. Recently, Zeng et al. [6], have proposed four electrochemical impedance models for the responses of Pt, Ni_3Al and FeAl in molten-salt systems at the open-circuit potential. Zeng [6] concluded that for Pt in molten $(Li, K)_2CO_3$ at 650°C the charge transfer was the rate limiting process; the corrosion of Ni_3Al in $(Li, Na, K)_2SO_4$ at 700°C presented characteristics of a diffusion-controlled reaction owing to the formation of non-protective scale, and for FeAl, the data presented different behavior with time, initially being influenced by a diffusion rate-controlling process from the observance of double capacitance loops at the beginning due to formation of protective scale. In this work, the hot corrosion resistance of IN 718 was evaluated by EIS from 588°C to 900°C in order to ascertain the possible mechanisms controlling the rate of corrosion processes in Na_2SO_4, $80V_2O_5$-$20Na_2SO_4$, $NaVO_3$, and natural ash.

2. EXPERIMENTAL

Test samples of IN 718 alloy were prepared from a stock of mill-certified IN 718 rod (see Table 1, for alloy composition).

Table 1. Chemical composition of 718 alloy (% wt)

Ni	Cr	Fe	Nb	Mo	Ti	Al	Mn	Si	Cu	C
54.21	19.13	17.64	4.50	3.09	0.85	0.21	0.05	0.25	0.03	0.04

Cylindrical specimens of 7mm diameter and 15 mm length were cut and polished with grit paper up to grade 800. The samples were then degreased well with acetone and then rinsed with ethanol. After drying, the specimens were stored in polyethylene zip-lock bags. The details of the experimental set-up for the electrochemical cell used in this work are given elsewhere [7]. Basically, the cell is composed of a quartz crucible 60 mm in height and 21.6 mm in internal diameter. Important elements here are: a) a reference electrode made of a platinum wire of 0.5 mm in diameter inside a quartz tube in contact with the molten salt of study (several other reference electrodes systems were tested, but this one gave the best stability response); b) an auxiliary electrode made of a platinum wire of 0.5 mm in diameter inside a mullite tube and filled with a refractory cement, and c) a IN 718 working electrode inside a mullite tube and filled with the same cement.

Table 2. Melting point of the work salts

Salts	Melting Point
Na_2SO_4	892ºC
$NaVO_3$	629ºC
80 wt%V_2O_5-20 wt%Na_2SO_4	587ºC
Natural Ash (V_2O_5, $Na_2O.V_2O_4.5V_2O_5$ and NaV_6O_{15})	756ºC

In order to obtain electrical contact with the IN 718 working electrode a stainless steel wire (sheathed in the mullite tube) was spot welded. A thermocouple sheathed with a quartz tube was immersed inside the test environment to monitor the temperature of each test. The corrosive atmosphere in the sealed cell was composed of Na_2SO_4, $80V_2O_5$-$20Na_2SO_4$, $NaVO_3$, or natural ash with melting points of 892°C, 587°C, 629°C and 756°C, respectively (see table 2) and static air. A furnace capable of reaching 1100°C was used for all the tests. Impedance measurements were taken 0.5 hours after the corrosion potential was stabilized. The range of used frequencies was from 10 KHz up to 0.001 Hz, and the amplitude wave of excitement signal was of ±10 mV with respect to the free corrosion potential. The temperatures used were 892°C, 587°C, 629°C and 756°C. After exposure to the environment, selected specimens were mounted and polished to be observed and analyzed in the Scanning electronic microscope (SEM).

3. RESULTS AND DISCUSSION

Figure 1 shows the electrical resistivity, Re, of Na_2SO_4, $NaVO_3$, $80V_2O_5$-$20Na_2SO_4$, and natural ash as a function of temperature.
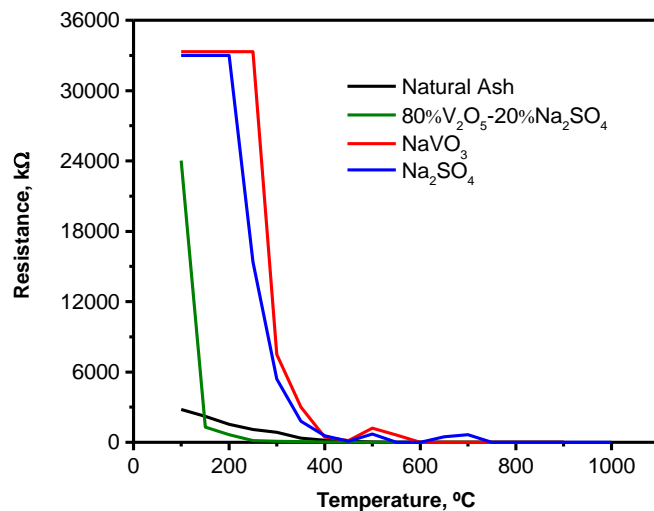
Figure 1. Resistivity of Na_2SO_4, $NaVO_3$, $80V_2O_5$-$20Na_2SO_4$ and natural ash a function of temperature

The Re values fall sharply when the temperature is increased from 500°C to 900°C. Above 750°C the resistivity was constant with a value of about 5 k-ohms. It is known that the lower the resistivity the higher the conductivity. This is important in order to obtain good electrical response.
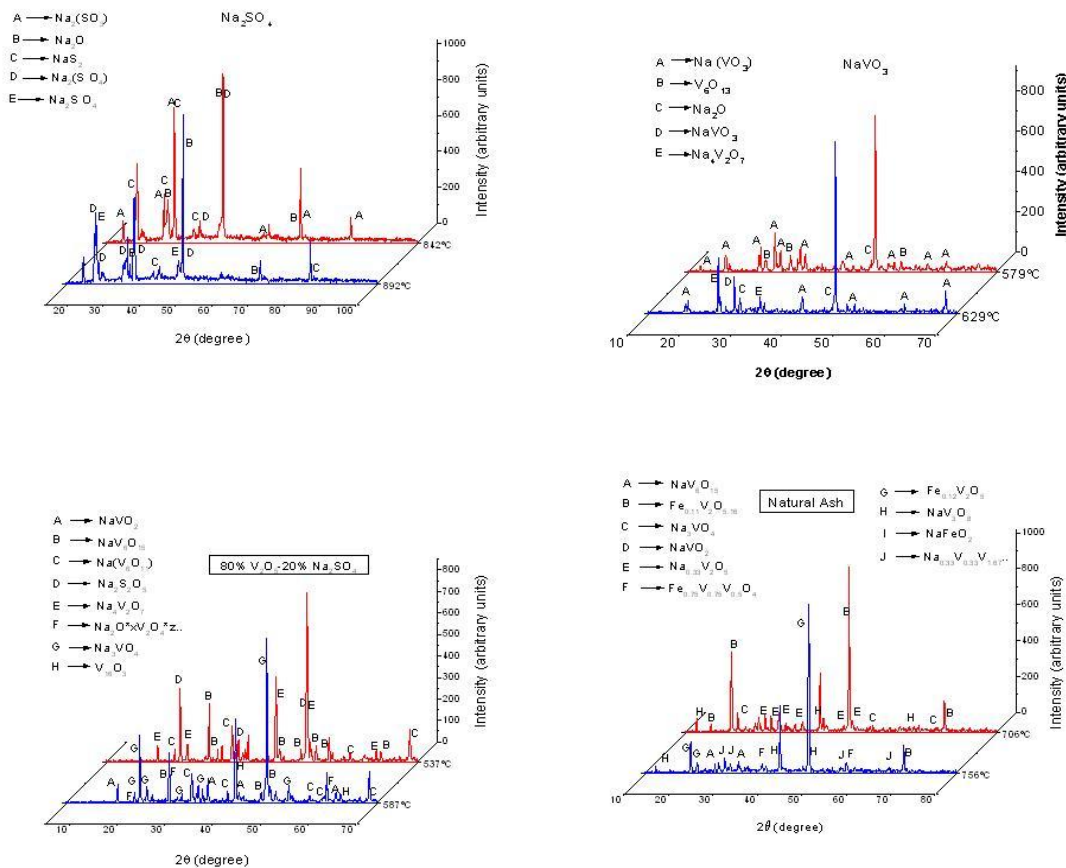
Figure 2. X-ray diffraction on the work salts.

The test salts (Na_2SO_4, $NaVO_3$, $80V_2O_5$-$20Na_2SO_4$, and natural ash) were identified by X-ray diffraction with the X-ray diffractometer Siemens D5000. This analysis was carried out at the respective melting point temperatures, and at 50 °C below each respective melting point of the relative salt. The aim of the X-ray diffraction was to identify the possible compounds that are generated at high temperatures for each salt and discern which compounds are more aggressive.

Table 3. Compounds found by X-ray diffraction on the work salts at different temperatures.

Salt	Temperature °C	Compounds
Na_2SO_4	842	$Na_2(SO_3)$, Na_2O, NaS_2, $Na_2(SO_4)$
	892	Na_2O, NaS_2, $Na_2(SO_4)$, Na_2SO_4
$NaVO_3$	579	$Na(VO_3)$, V_6O_{13}, Na_2O
	629	$Na(VO_3)$, Na_2O, $NaVO_3$, $Na_4V_2O_7$
$80V_2O_5$-$20Na_2SO_4$	537	NaV_6O_{15}, $Na(V_6O_{11})$, $Na_2S_2O_5$, $Na_4V_2O_7$
	587	$NaVO_2$, NaV_6O_{15}, $Na(V_6O_{11})$, $5Na_2O \cdot V_2O_4 \cdot 11V_2O_5$, Na_3VO_4, $V_{16}O_3$
Natural Ash	706	$Fe_{0.11}V_2O_{5.16}$, Na_3VO_4, $Na_{0.33}V_2O_5$
	756	NaV_6O_{15}, $Fe_{0.11}V_2O_{5.16}$, $Fe_{0.75}V_{0.75}V_{0.5}O_4$, $Fe_{0.12}V_2O_5$, NaV_3O_8, $Na_{0.33}V_{0.33}V_{1.67}$

Figure 2 shows the diffraction patterns and the identified compounds after heating salts under static air in the range of temperature of this study. Intensities correspond to compounds with a great variety of stoichiometries, as is shown in table 3. In the case of $NaVO_3$, $80V_2O_5$-$20Na_2SO_4$ and natural ash salts Intensities correspond to compounds of stoichiometry of $Na_2O \cdot V_2O_4 \cdot V_2O_5$ and $5Na_2O \cdot V_2O_4 \cdot 11V_2O_5$. In previous studies, it has been demonstrated that the corrosiveness shown by the different types of vanadates compounds is a function of its oxygen absorption capacity [8,12]. Particularly, two identified phases, $Na_2O \cdot V_2O_4 \cdot V_2O_5$ and $5Na_2O \cdot V_2O_4 \cdot 11V_2O_5$ are found among the vanadium compounds with the greatest oxygen absorption capacity as it is observed of the results of Greenert [14]. Cunningham and Brasunas [13], who reported that the $Na_2O \cdot V_2O_4 \cdot V_2O_5$ compounds are more corrosive than the $5Na_2O \cdot V_2O_4 \cdot 11V_2O_5$. Thus, the presence of these compounds will increase the corrosiveness of the salt.

Fig.3 a) shows the Nyquist plots obtained for IN 718 in pure Na_2SO_4 at the different temperatures. At 50° C below the melting point, 842° C, a capacitive-like, depressed semicircle can be observed at high frequencies but at low frequencies both the real and imaginary parts describe a straight line, indicating that the corrosion process is under a mixed control: by charge transfer at high

frequencies, and by diffusion control at low frequencies, diffusion of the aggressive species through the salt layer which is not melt.
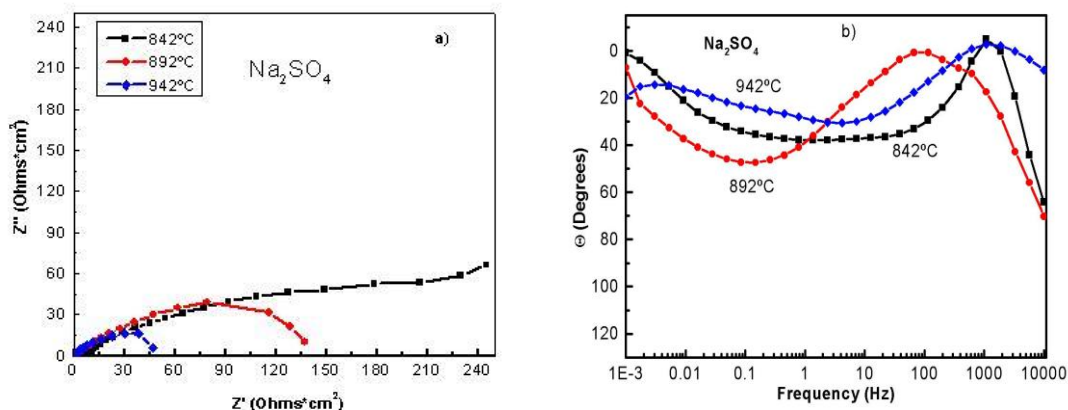
Figure 3. Impedance diagram for IN 718 immersed in Na_2SO_4 at different temperatures in the a) Nyquist and b) Bode representation.

As the salt temperature is increased, the impedance data describe depressed, capacitive-like semicircles, with their axis in the real axis, and with their diameter decreasing as the temperature increases. This is due to the fact that at these temperatures the working salt is melted, so the diffusion of ions through it is much easier and their transport is the rate controlling step and there is now an increased mobility of ionic charge carriers [8].The diameter of the semicircle is associated with the polarization resistance and thus the corrosion rate; the larger the semicircle diameter, the lower the corrosion rate.
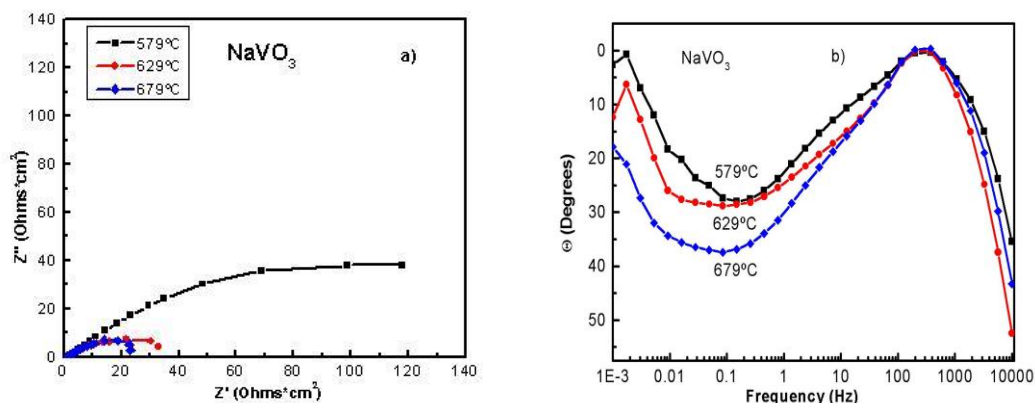
Figure 4. Impedance diagram for In 718 immersed in $NaVO_3$ at different temperatures in the a)Nyquist and b) Bode representation

Thus, we can see that the corrosion rate increases with temperature. On the other hand, Fig. 3 b) shows the Bode diagram in the Phase angle-frequency format. It can be seen that there is one peak

at 1000 Hz for 842 and 942°C and at 100 Hz for 892°C. The presence of only peaks means that no protective film is formed at any temperature and this is the reason of the increase in the corrosion rate with temperature.

Fig. 4 a) shows the impedance data in the Nyquist format for IN 718 superalloy exposed to NaVO$_3$ at its melting temperature (629°C), 579 and 679°C.This figure shows that the impedance data describe capacitive-like, depressed semicircles, with its axis in the real axis. The semicircle diameter decreases as the temperature increases, indicating that the corrosion rate increases with temperature. The shape of the semicircle indicates that the corrosion process is under charge transfer control. The Bode diagram in this case, Fig.4 b), shows only one peak around 300 Hz regardless the working temperature, indicating that there is not the formation of a protective layer, since, in this case, a second peak should have been observed at a different frequency.
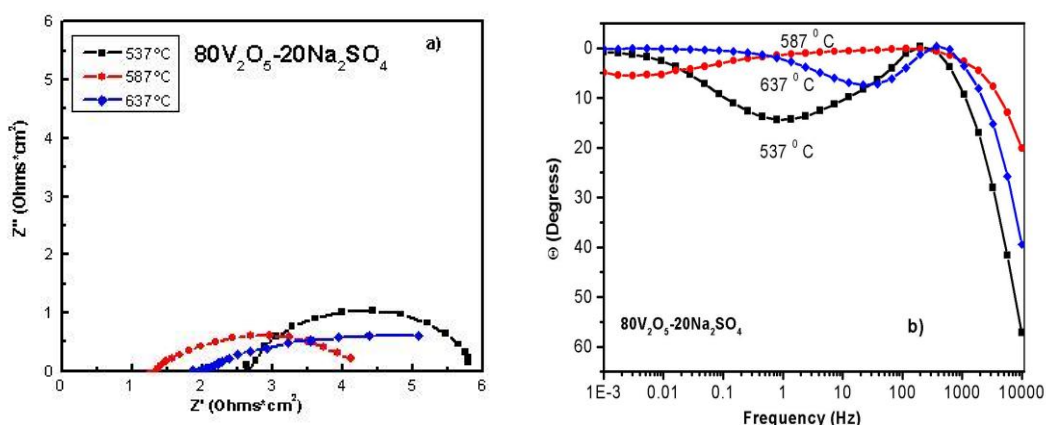
Figure 5. Impedance diagram for IN 718 immersed in the 80V$_2$O$_5$-20Na$_2$SO$_4$ mixture at different temperatures in the a)Nyquist and b) Bode representation.

When superalloy IN 718 was exposed to the 80V$_2$O$_5$+20Na$_2$SO$_4$ mixture at its melting temperature (587°C) 637 and 687°C, the Nyquist data describe, once again, capacitive-like, depressed semicircles, with its centre in the real axis, Fig. 5 a). Dislike the previous cases, this time the semicircle diameter increased when the temperature increased, indicating that the corrosion rate decreased with temperature. The Bode diagram, Fig. 5 b), showed only one peak around 300 Hz at 537°C, but at 637 and 687°C, there seems to be a superposition of two peaks: one at 300 Hz and another one around 1 Hz. The existence of two peaks means that a protective salt layer has been formed on the alloy surface, which could explain the increase in the semicircle diameter in the Nyquist diagrams, and thus, a decrease in the corrosion rate as temperature increases.

Finally, Fig. 6 a) shows the Nyquist diagram for In 718 exposed to the natural ash at 706, 756 (meeting point) and 806°C. It can be seen that, at 706, 756°C, the data describe a small, high frequency, capacitive-like semicircle and a large low frequency semicircle, with their centers at the real axis and with diameter decreasing with the temperature. The emergence of a large capacitive low frequency semicircle may be related to the formation of a protective scale on the alloy surface. At 806°C, only a semicircle is observed. Thus, it can be seen that the corrosion rate decreases as the

temperature increases. The Bode diagram, Fig. 6 b), showed only one peak around 300 Hz at 537°C, but at 637 and 687°C, there seems to be a superposition of two peaks: one at 300 Hz and another one around 1 Hz. The existence of two peaks means that a protective salt layer has been formed on the alloy surface, which could explain the increase in the semicircle diameter in the Nyquist diagrams, and thus, a decrease in the corrosion rate as temperature increases.
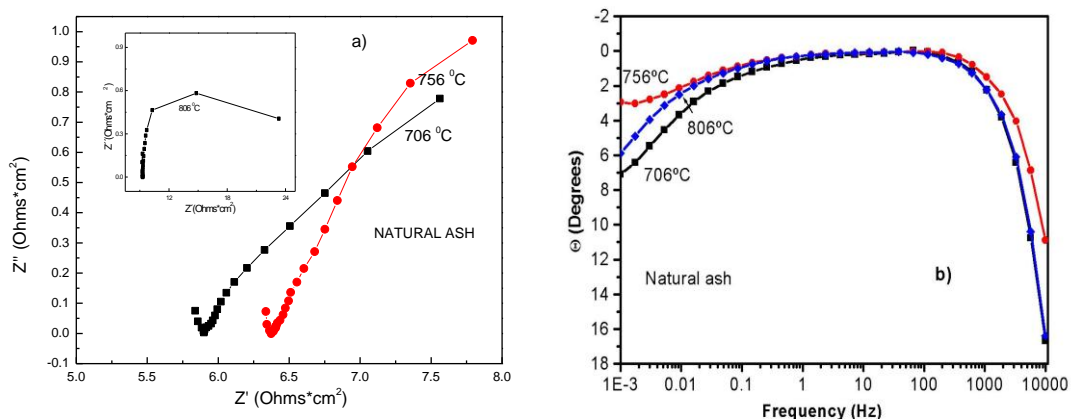
Figure 6. Impedance diagram for In 718 immersed in natural ash at different temperatures in the a)Nyquist and b) Bode representation.
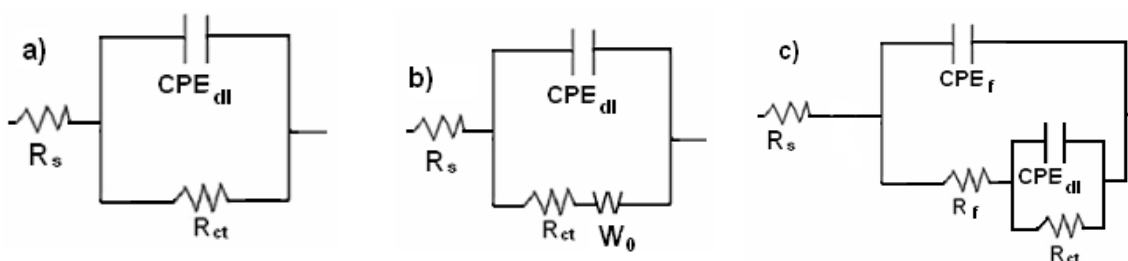
Figure 7. Equivalent electric circuits to simulate the EIS results for IN 718 exposed to molten salts when the corrosion process is a) under charge transfer control, b) when it is under charge transfer and diffusion control, and c) when the alloy is covered with a protective salt layer.

Electric circuits can be used to simulate impedance data (table 4). Thus, the following elements are to be expected in the equivalent circuit model: R_f represents the resistance of the salt layer, C_f is its capacitance in parallel; R_{ct} represents the charge transfer resistance; W represents the Warburg impedance and C_{dl} represents the double layer capacitance; finally, R_s represents the salt resistance. However, one has to account for the inhomogeneity of the salt film coating system. When a non-ideal frequency response is present, it is commonly accepted to employ distributed circuit elements in an equivalent circuit. The most widely used is constant phase element (CPE), which has a non-integer power dependence on the frequency. The impedance of a CPE is described by the expression:

$$Z_{CPE} = Y^{-1} (jw)^{-n} \qquad\qquad (1)$$

Where Y is a proportional factor, j is $\sqrt{-1}$, w is $2\pi f$ and n has the meaning of a phase shift [15]. Often CPE is used in a model in place of a capacitor to compensate for non-homogeneity in the system. This created the overall equivalent circuit model shown in Figure 7

Table 4. Circuit parameters used for the simulation of the impedance data

Salt	Temperature (°C)	R_s ($\Omega \cdot cm^2$)	R_{ct} ($\Omega \cdot cm^2$)	C_{dl} (F)
Na_2SO_4	842	8.16	311.0	0.00906
Na_2SO_4	892	1.09	145.8	0.012
Na_2SO_4	942	0.62	48.8	0.173
$NaVO_3$	579	2.30	193.0	0.044
$NaVO_3$	629	2.32	34.7	0.051
$NaVO_3$	679	1.41	23.7	0.118
80 wt%V_2O_5+20 wt%Na_2SO_4	537	2.62	3.25	0.021
80 wt%V_2O_5+20 wt%Na_2SO_4	587	1.30	3.3	0.14
80 wt%V_2O_5+20 wt%Na_2SO_4	637	1.91	5.4	0.647
Natural Ash	706	5.89	4.1	3.74
Natural Ash	756	6.39	4.9	7.23
Natural Ash	806	9.21	6.5	0.157

Figure 8 shows a micrograph of IN 718 corroded in pure Na_2SO_4 at 892°C together with elemental energy dispersive spectroscopy (EDS) mappings of Cr, O, Fe, Ni and S. It can be noticed that Cr and O are mainly distributed outside the alloy, perhaps forming a chromium oxide, Cr_2O_3 layer, and that sulphur has penetrated into the alloying, producing internal sulphides. Something very similar can be observed for IN 718 exposed to the natural ash at 756°C, Figure 9, where the distribution of Cr and O outside the alloy is evident, forming, perhaps, a Cr_2O_3 later, which has been dissolved by the molten ash, since the presence of vanadium inside the alloy is notorious.

As it can be seen on the X-ray mappings shown on Fig. 9, this oxide layer corresponds to a corrosion product formed mainly by O, Cr and V, and it may be to a compound including chromium oxide Cr_2O_3, the most common oxide found in Cr-containing alloys at high temperature, and a V-containing compound. Because the corrosion reactions in molten salts are controlled by a process of oxidation of the metal and reduction of the salts, the relative activity of the molten salts with the metal is important, since the corrosion potential of the metal frequently is controlled by the impurities in the molten salt or gas phase, which increases the rate of cathodic reaction or in the change of the basicity or acidity of the molten mixture. These could make the dissolution of the adherent scale on the metal. The dissolution can be taken by two mechanisms, either by local dissolution or by selective dissolution

of the different components of the oxide. In the first case, the growth of the protective oxide will be smaller than in the case of gas corrosion, and the resulting corrosion rate will be bigger.
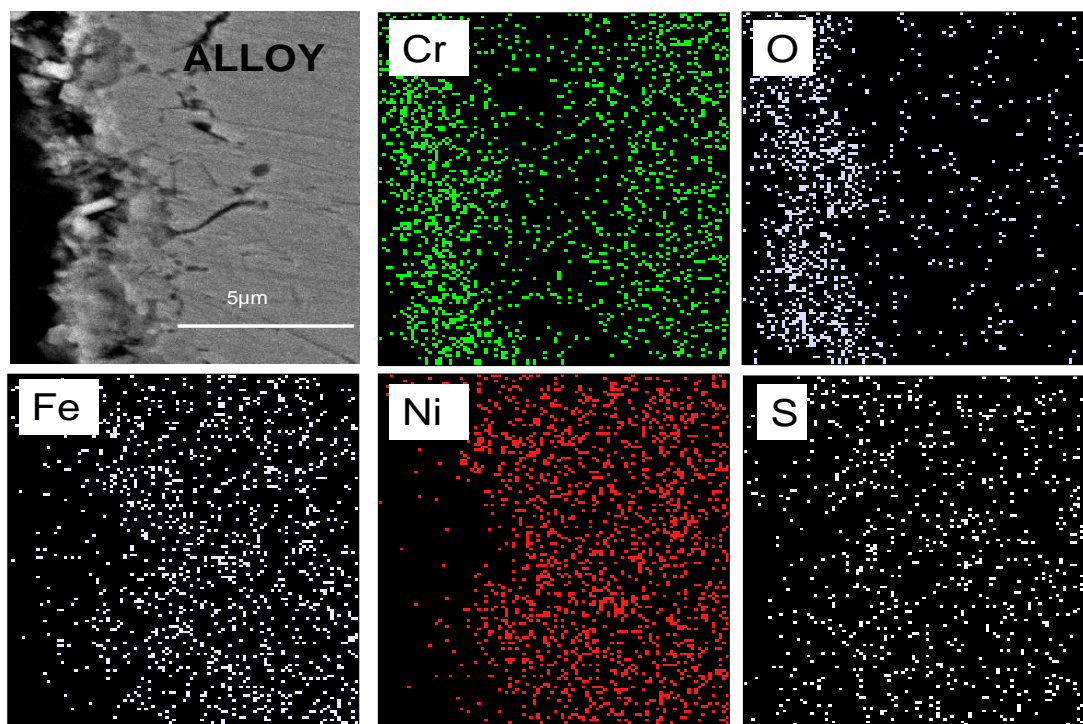
Figure 8. SEM image of IN 718 corroded in Na_2SO_4 at 892 ∘C and EDS map of Cr, O, Fe, Ni and S.

For the other case, if selective dissolution takes place, then the structure and integrity of the scale is damaged by the loss of some elements or components and it is manifested with cracking and spalling of the scale.

For Cr, the main compounds included both chromium vanadates and chromium oxides, but some other compounds were found such as Fe_2O_3 and NiO. These compounds could have been formed according to next equations:

$$Fe2O3 \; + \; 2\,NaVO3 \; = \; 2\,FeVO4 \; + \; Na2O \tag{2}$$

$$3\,NiO \; + \; 2\,NaVO_3 \; = \; Ni_3(VO_4)_2 \; + \; Na_2O \tag{3}$$

$$Cr_2O_3 \; + \; 2\,NaVO_3 \; = \; 2\,CrVO_4 \; + \; Na_2O \tag{4}$$

where the main ion is metavanadate (VO_3^-), which comes from the dissolution of $NaVO_3$. However, when V_2O_5 is the corrosive agent, the metavanadate ion is present and the dissociation of V_2O_5 is according to:

$$M_2O_3 \; + \; V_2O_5 \; = \; 2\,MVO_4 \tag{5}$$

Based on this, the dissolution of protective oxides can be explained as:

$$
\begin{array}{c}
\underset{\mathrm{O}}{\overset{\mathrm{O}}{\diagdown}}\!\!\!V\!-\!\mathrm{O}^{\ominus} \\[2mm]
+ \\[2mm]
\underset{\mathrm{O}}{\overset{\mathrm{O}}{\diagdown}}\!\!\!V^{\oplus}
\end{array}
\quad
\begin{array}{c}
\overset{\mathrm{O}}{\underset{\oplus}{\parallel}}M \\[2mm]
\\[2mm]
\ominus\mathrm{O}\!-\!\underset{\mathrm{O}}{\overset{\parallel}{M}}
\end{array}
\quad = \quad
2\left(\underset{\mathrm{O}}{\overset{\mathrm{O}}{\diagdown}}\!\!\!V\!-\!\mathrm{O}\!-\!M\!=\!\mathrm{O}\right)
$$
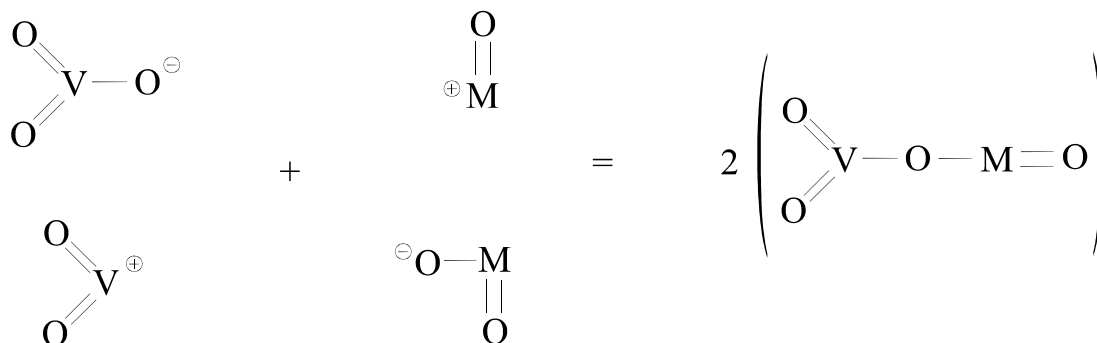
Thus, the dissociation of V_2O_5 allow us to explain the increase in the corrosion rate due to the fact that the species involved in the corrosion process are metavanadate ions, produced by the dissociation of $NaVO_3$ according to equations 2, 3 and 4, which do not depend upon the salt basicty, and metavanadate ions and VO_2^+ cation due to the dissociation of V_2O_5, according to equation 5, which do not depend upon the salt basicity.
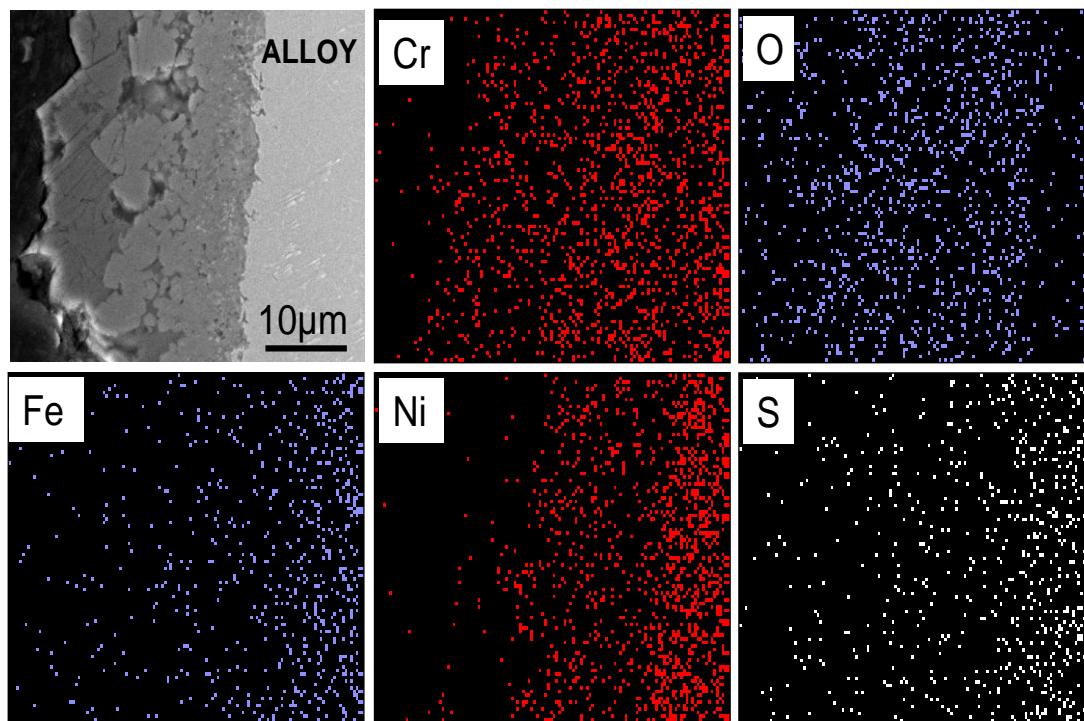
Figure 9. SEM image of IN 718 corroded in Natural ash at 756°C and EDS maps of Cr, O, Fe, Ni, V

These dissolution reactions could have been destroyed the formed oxides on the alloy surface and induced its destruction at high temperatures. The presence of Na_2SO_4 changes the salt basicity, since this salt has two components: Na_2O (basic) and SO_3 (acidic), the melting point of the mixture, and the corrosion rate. In addition, the presence of sulfur increases the corrosion rate since now there is

a new phenomenon, the sulfidation of the alloy. Na_2SO_4 dissolves any formed oxide, either by basic or acidic dissolution, releasing sulfur, which penetrates into the metal, producing internal sulfidation, increasing the corrosion rate.

Based on the above analysis, the corrosion process of IN 718 superalloy into the molten salts may be summarized as follows: the hot corrosion occurred by oxidation of Ni and Cr at the anodic site and formed Ni^{2+} (NiO) and Cr^{3+} (Cr_2O_3) ions, while at the cathodic site O_2 is reduced to O^{2-} and V^{5+} to V^{4+}. Metal ions like Ni^{2+} and Cr^{3+} react with the oxide ions to form the metal oxides. As a result, the oxygen concentration was increased at the surface of the metal and then oxygen diffused inward and formed oxides. Metal oxides detected by X-ray diffraction are a clear indication of electrochemical reactions during the hot corrosion process. The presence of VO_2 indicates that vanadium has been reduced from V^{5+} in the $NaVO_3$ salt to V^{4+}, and it is a strong evidence that the proposed cathodic reaction is taking place, and, therefore It proves, again that hot corrosion of IN 718 alloy is electrochemical in nature. Probably the Cr_2O_3 layer reacted with V and formed a compound, to which C_{ox} and R_{ox} represents. In a series array, a smaller semicircle in the Nyquist plot at high frequency was associated to the alloy corrosion resistance mainly due to activity in the metal scale interface (given by C_{dl} in parallel with R_t).

4. CONCLUSIONS

The Nyquist plots, in general, present processes in which the activation, charge transfer mechanism was dominant, with the exception of Na_2SO_4 at 842°C and 679°C for $NaVO_3$ where, in addition to the activation there is also diffusion.

The least aggressive salt was the synthetic Na_2SO_4 salt at temperature of experimentation, while the most aggressive was in the presence of $80V_2O_5$-$20Na_2SO_4$ salt.

The corrosion rate, of Na_2SO_4 and $NaVO_3$, increases with increasing temperature around the melting point.

By contrast, in $80V_2O_5$-$20Na_2SO_4$ and natural ash, as the temperature rises around the melting point, the corrosion rate decreases. This is due to a change in the basicity or acidity of the salt due to the presence of different ions (VO_3^-, Na_2O, SO_3, etc.) which increase the salt corrosivity.

References

1. D. M. Farrell, W.K. Cox, F.H. Stott, D.A. Eden, J.L. Dawson and G.C. *Wood, High Temp. Technol., Feb.* (1985), 16-21.
2. G. Gao, F.H. Stott, J. L. Dawson and D.M. Farrell, *Oxid. Metals*, 33, (1990), p.79.
3. Y.M. Wu and R.A. Rapp,   *J. Electrochem. Soc.*, Vol. 138, (1991), pp.2683-2690.
4. C.Xiang Wu, A. Nishikata and T. Tsuru, *High Temper. Advanc. Mater. and Protec. Coat.*, (1992), pp.221
5. Y.M Wu, *Electrochem. Soc*. Vol. 138 (1991), pp. 2342
6. C.L. Zeng, W. Wang, W.T. Wu, *Corros. Sci.* Vol. 43 (2001), p.p. 787
7. F.M. Almeraya-Calderon. Ph. D. Thesis. Centro de Investigación en Materiales Avanzados. S. C., Chihuahua, Chi, México. 1998.
8. D. M. Farrell, W.K. Cox, J.L. Dawson, P.D.W. Bottomley, UK Corrosion 89, Blackpool, UK (1989).
9. D. M. Farrell, F.H. Stott, G. Rochinni, and A. Colombo, *Mat. High Temp*., Vol. 10, No.1, (1992), pp11
10. S. Gitangaly, S. Prakash, S. Sing, *Brit. Corrosion J*., Vol.37, No.1, (2002), pp 56
11. U. Rammelt, L.M. Duc, W. Pleith *J. Appl. Electrochem*. 35(2005) 1225
12. A.Wong-Moreno, Y. Mujica-Martinez, L. Martinez, Corrosion '94, NACE International Paper 185, 1994, p. 185/1.
13. G.W. Cunningham, A.de S. Brasunas, *Corrosion* 12 (1956) 389t.
14. W.J. Greenert, *Corrosion* 18 (1962) 575.
15. C.L. Zenga,, J. Li., *Electrochimica Acta*. 50 (2005) 5533–5538
16. Abdel Salam Hamdy, E. El-Shenawy and T. El-Bitar. *Int. J. Electrochem. Sci*., 1(2006)171-180.